

VT/VF risk in animal model of hypertensive heart disease predicted by distribution of patchy fibrosis

Supporting Image and Cell Segmentation Information

Prashanna Khwaounjoo,^{1,2} Gregory B. Sands,¹ Ian J. LeGrice,^{1,3} Girish Ramulgun,^{1,4}
Jesse A. Ashton,¹ Johanna M. Montgomery,³ Anne M. Gillis,⁵ Bruce H. Smaill,¹
Mark L. Trew¹

¹Auckland Bioengineering Institute, University of Auckland, Auckland, New Zealand; ²Department of Anatomy, University of Otago, Dunedin, New Zealand; ³Department of Physiology, University of Auckland, Auckland, New Zealand; ⁴IHU-Liryc, University of Bordeaux, Bordeaux, France; ⁵Libin Cardiovascular Institute of Alberta, University of Calgary, Calgary, AB, Canada.

Anatomical measurements and fibrosis distribution

Tiled images of wheat germ agglutinin-conjugated AF488 (WGA)-labeled short axis sections of rat heart were combined with ImageJ (imagej.nih.gov) to create a single image. Figure 1A shows an example from an 18 month animal. Initial segmentation of tissue from non-tissue used a binary filter to obtain a mask for the short axis slice (Figure 1B). Measurements were taken of the average thicknesses of the LV and RV (Figure 1B) and lumen area and lumen centroid (Figure 1C).

Cell membranes and the extracellular matrix are labeled by WGA. Greater image intensity within the boundary mask indicates the presence of fibrosis (Figure 1A), while the spatial distribution of this signal provides information on the nature and extent of this fibrosis. Using a maximum entropy intensity filter¹ the higher intensity pixels were segmented to differentiate the regions of fibrosis from the rest of the tissue and create a mask (Figure 1D). This filter was chosen as it was able to duplicate the histogram based WGA fibrosis segmentation from Emde et al. (2014).² For all hearts, the total segmented area of fibrosis was normalised with respect to short-axis area to determine the fibrotic percentage.

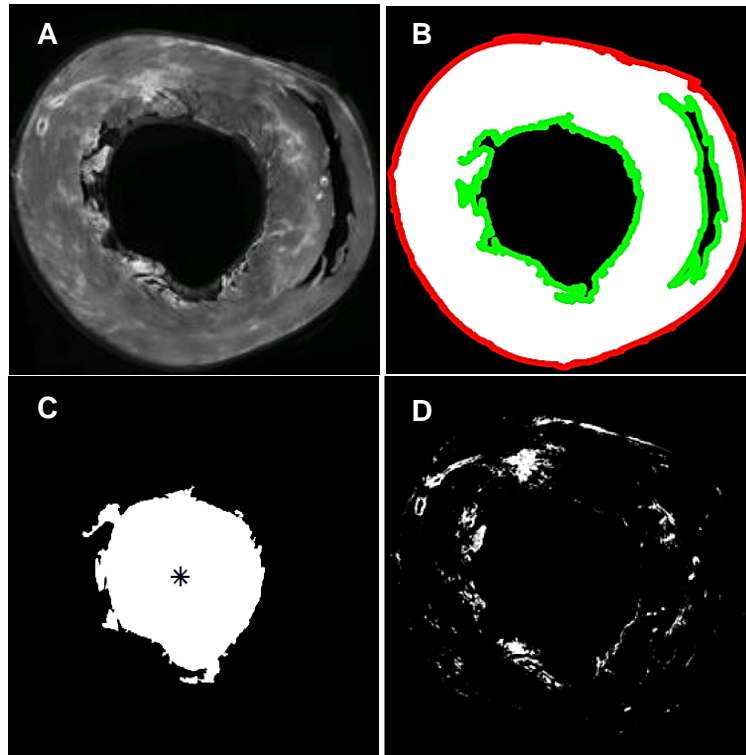


Figure 1. Short axis slice representation and measurements. **A.** Merged WGA stained short axis slice (higher intensity pixels indicate fibrosis) **B.** Tissue segmentation (white), endocardial (green) and epicardial (red) coordinates **C.** LV cavity with centroid highlighted by asterisk. **D.** Segmented patches of fibrosis.

To quantify and compare the distribution of fibrosis across all hearts, the segmented mask (Figure 1D) was translated into a polar coordinate system. For each separate individual patch in the mask (i.e. a patch of fibrosis – based on the WGA intensity signal), the patch centroid and area were computed. The centroid position was mapped into a polar coordinate system based on its polar angle and transmural (wall thickness) location relative to the lumen centroid (Figure 2A). A polar angle of 0° was defined as mid septum and 90° to 270° were the LV free wall. In the transmural field 0 was the endocardium and 1 the epicardium. Local “densities” of the patches were then determined by discretizing the spatial field into 50 by 50 bins. The resultant field was smoothed using a 2D histogram filter³ to create a “heat map” (Figure 2B).

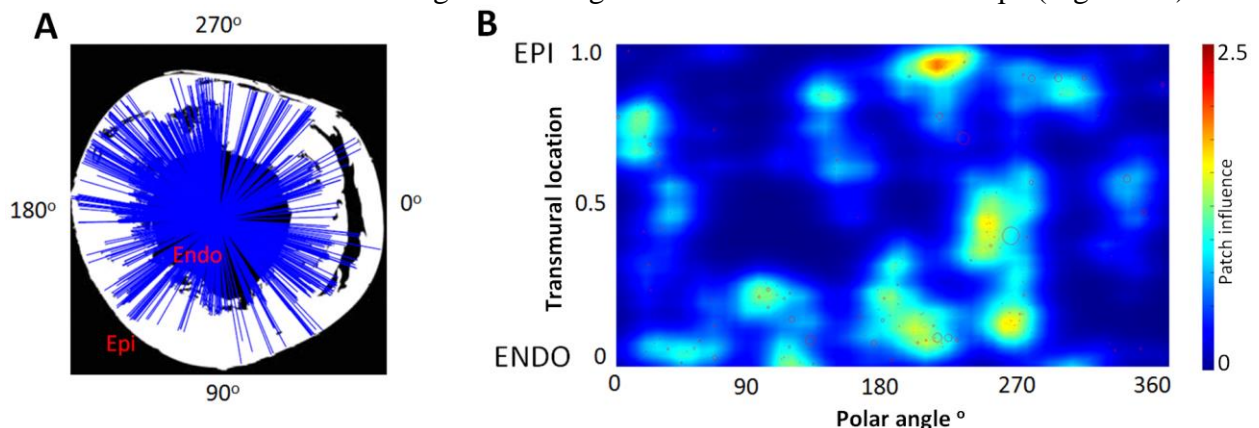


Figure 2. Fibrosis patch distribution and density. **A.** Intramural location of patches of fibrosis relative to LV cavity centroid. Blue lines indicate identification of patch from cavity centre. **B.** Heat map of fibrosis patch density in the polar coordinate system. Colour scale indicates influence of patch of fibrosis. Red indicates the influence of 2.5 or more patches and dark blue indicates no fibrotic influence.

The heat map was resampled to 100×360 pixels in the transmural and polar angle axes respectively. A threshold (using a value of 1, representing the influence of one patch) was applied to the resampled “heat map” image to quantify the influence of fibrosis patch density and extract the connected high-density regions. These aggregated regions of fibrosis patches from the heat map in Figure 2B are shown in Figure 3A as white regions. The regions were skeletonized, using the MATLAB® `bwskel*` function, as shown in Figure 3B and Figure 3C. The area of the region with the longest skeletonization (a measure of fibrotic patch density tortuosity and, hence, possible reentrant path length – referred to as the aggregated fibrosis patch density length (AFL)) was normalized across all hearts in the study giving an index between 0 and 1. This is the aggregated fibrosis patch density area (AFA) index.

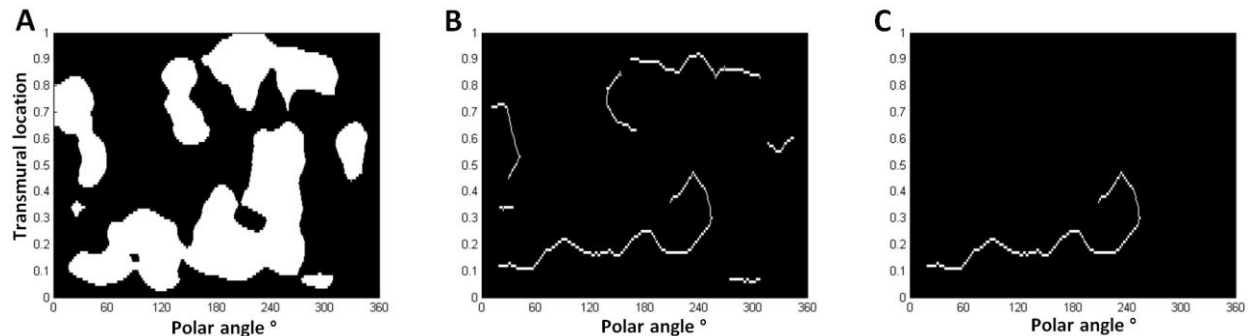


Figure 3. Mask of connected regions of fibrosis and measurements. **A.** Mask of connected regions of fibrosis (threshold of 1) **B.** Skeletonised lengths of each separate contiguous region of the mask **C.** Maximum path length of the skeletonised lengths.

This method for assessing the aggregation of fibrosis patch density in cardiac tissue ensures that the structure of the fibrotic patch distribution is correctly accounted for. Fibrotic structures as barriers to coordinated activation would not be fully captured by just a maximum area measure, for example. Our fibrotic consolidation measure includes both path length and area, and holds similarities to a measure of tortuosity in 2D discontinuous myocardium that was developed and used in the analysis of Engelman et al. (2010).⁴

Typical examples of the spatial distributions and characteristics of fibrosis quantified using this method applied to LV short axis slices are shown in Figure 4. The dark areas in Figure 4A are regions of intense WGA fluorescence due to perimysial or replacement fibrosis. The heterogeneous distribution of these patches is highlighted in the polar distribution maps (Figure 4B) and the analysis of fibrotic regional connectedness is shown in Figure 4C.

Each high intensity pixel (darker pixels in Figure 4A) was also translated into the polar coordinate field to quantify the distribution of the amount of fibrosis. The resulting image was discretized into 10 and 12 segments for the transmural and polar axes respectively (Figure 5).

* mathworks.com/help/images/ref/bwskel.html

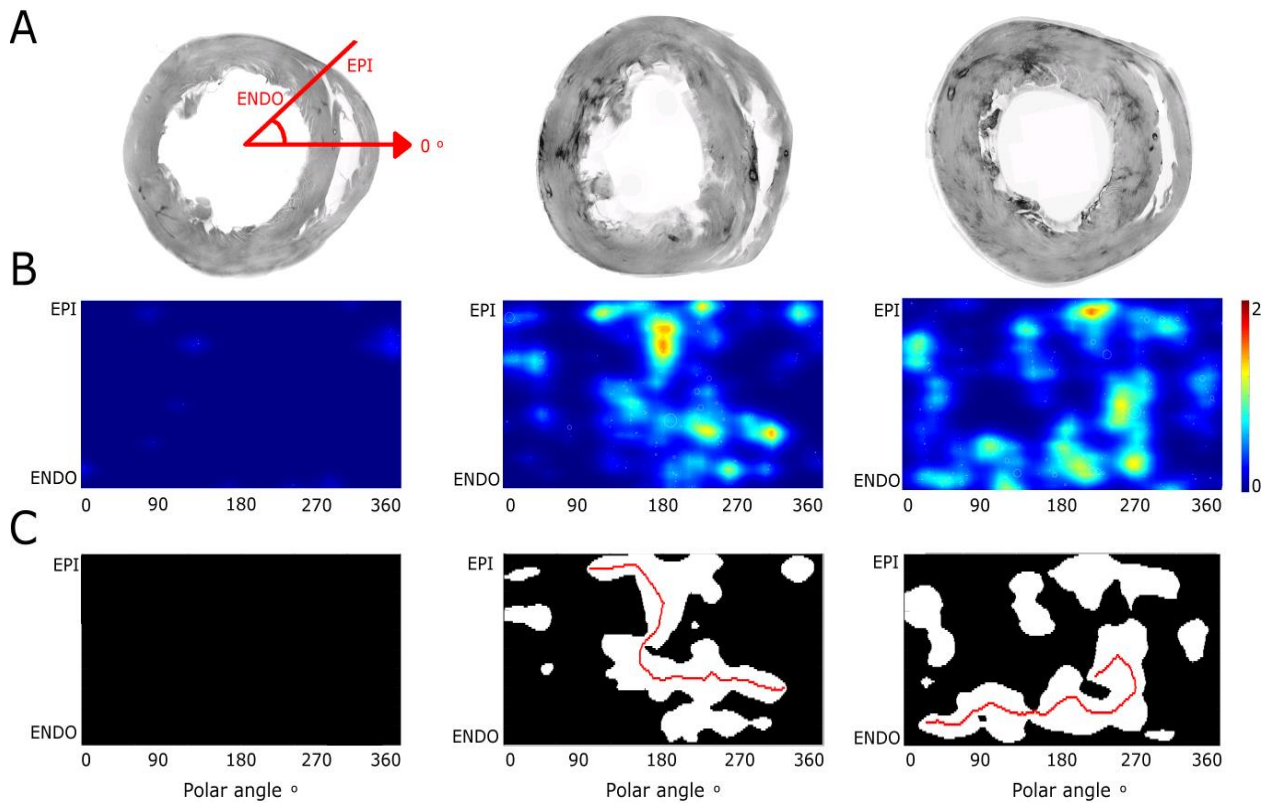


Figure 4. Typical distributions of WGA staining in LV short-axis sections at 6, 12 and 18 months. **A.** Initial LV sections, intensely dark regions stained are representative of patches of fibrosis. **B.** Polar heat maps reflect the intensity and regional extent and the distribution of patches of fibrosis. **C.** Characterisation of potentially connected regions of fibrosis (white). Maximum skeletonised lengths are indicated in red.

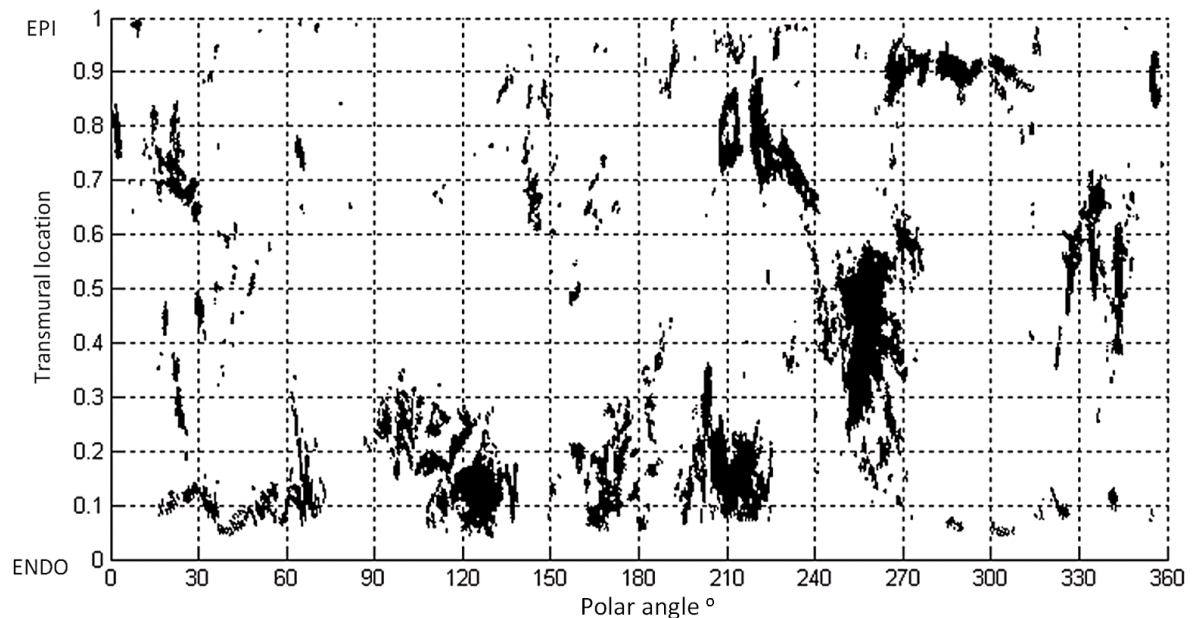


Figure 5. Distribution of fibrosis (individual high intensity pixels of WGA) in circumferential and transmural coordinate system. Transmural axes discretised into 10 sections of 0.1 units, while the circumferential axes have been discretised into 12 radial sections of 30°. These data are equivalent to data in figures 1, 2, 3 and 4 column 3.

Cellular organization and architecture

ITK SNAP (itksnap.org)⁵ was used to manually segment the high resolution cell data into individual cells (Figure 6). The segmentation was conducted by a contract operator with no link to the project and its potential findings (i.e. they were unaware of potential alterations to cell morphology with HHD progression). For each internal cell (i.e. a whole myocyte fully contained in the image volume) the longitudinal orientation was determined using the eigenvectors of the covariance matrix.⁶ The longitudinal axis and centre of mass of the cell were then used to determine the cell cross sectional area. Cell lengths and total cell volumes were also measured, while the surface areas were calculated using Minkowski measures.⁷ Distance maps from each internal (whole) myocyte were generated to identify/count all other myocytes within a distance of 1 voxel ($0.41 \mu\text{m}$) to the outer sarcolemma. This metric provided an estimate of likely cell coupling i.e. number of neighboring myocytes. The relative volume of the fibrosis was estimated from the WGA intensity using the ImageJ (imagej.nih.gov) implementation of the Shanbhag filter.

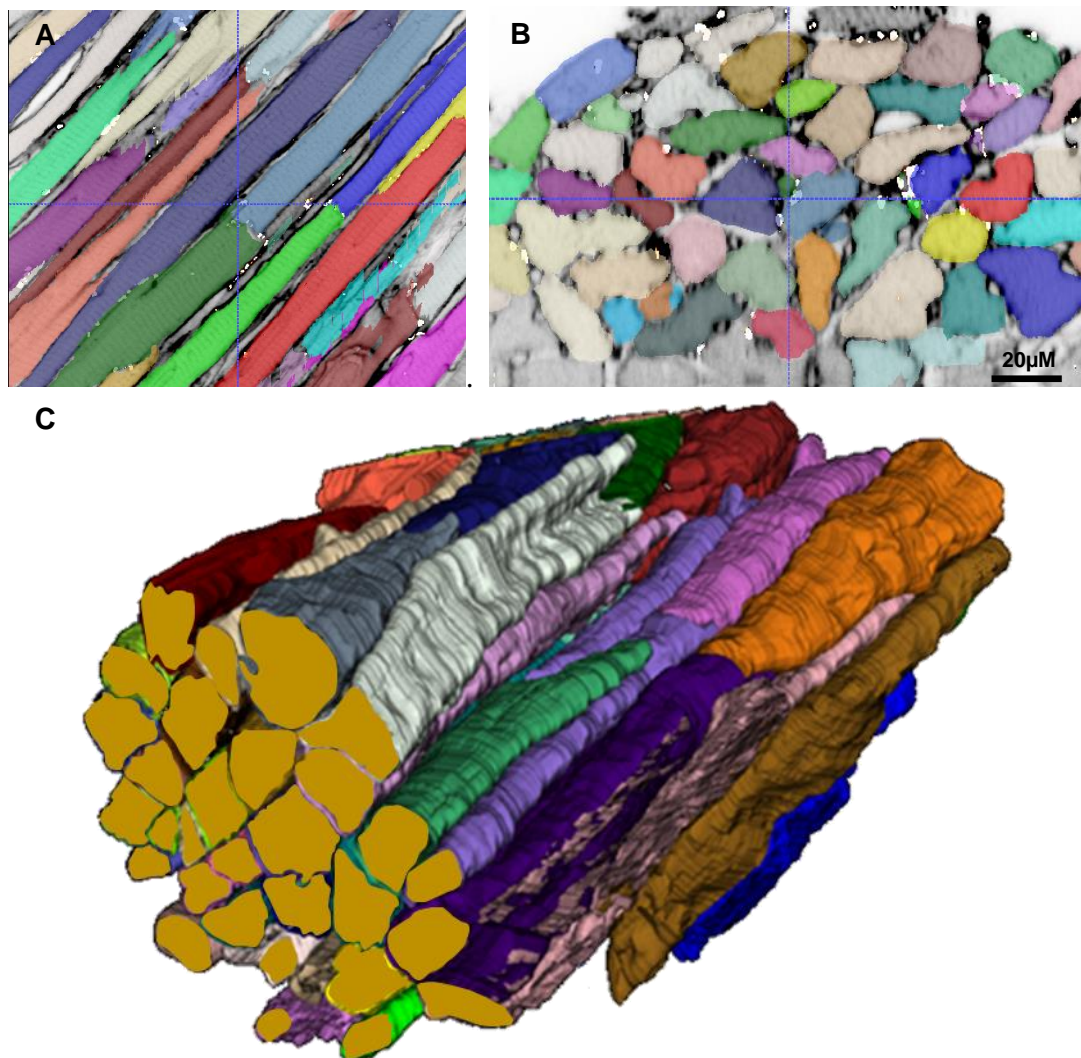


Figure 6. Cell segmentations using ITK SNAP. **A.** Axial slice of tissue volume. **B.** Side view of tissue section. **C.** 3D rendering of segmented cells. Cells not wholly in the image volume are identified by their truncation at the image boundaries.

References

1. Zheng X, Ye H, Tang Y. Image Bi-Level Thresholding Based on Gray Level-Local Variance Histogram. *Entropy*. 2017;19:191.
2. Emde B, Heinen A, Gödecke A, Bottermann K. Wheat germ agglutinin staining as a suitable method for detection and quantification of fibrosis in cardiac tissue after myocardial infarction. *Eur J Histochem*. 2014;58:2448.
3. Eilers PHC, Goeman JJ. Enhancing scatterplots with smoothed densities. *Bioinformatics*. 2004;20:623–628.
4. Engelman ZJ, Trew ML, Smaill BH. Structural heterogeneity alone is a sufficient substrate for dynamic instability and altered restitution. *Circ Arrhythm Electrophysiol*. 2010;3:195–203.
5. Yushkevich PA, Piven J, Hazlett HC, Smith RG, Ho S, Gee JC, Gerig G. User-guided 3D active contour segmentation of anatomical structures: Significantly improved efficiency and reliability. *Neuroimage*. 2006;
6. Reyment RA, Jvreskog KG. Applied Factor Analysis in the Natural Sciences. 1993.
7. Legland D, Kiêu K, Devaux M-F. Computation of minkowski measures on 2D and 3D binary images. *Image Anal Stereol*. 2011;26:83.